Nitric Oxide Binding to the Ferri- and Ferroheme States of Nitrophorin 1, a Reversible NO-Binding Heme Protein from the Saliva of the Blood-Sucking Insect, *Rhodnius prolixus*

Xiao D. Ding,[†] Andrzej Weichsel,[‡] John F. Andersen,[‡] Tatjana Kh. Shokhireva,[†] Celia Balfour,[‡] Antonio J. Pierik,[§,||] Bruce A. Averill,[§] William R. Montfort,*[,‡] and F. Ann Walker*[,†]

Contribution from the Departments of Chemistry and Biochemistry, University of Arizona, Tucson, Arizona 85721, and the E. C. Slater Institute, Faculty of Chemistry, University of Amsterdam, Plantage Muidergracht 12, 1018 TV Amsterdam, The Netherlands

Received August 19, 1998

Abstract: The recombinant NO-binding heme protein, nitrophorin 1 (NP1) from the saliva of the blood-sucking insect, *Rhodnius prolixus*, has been studied by spectroelectrochemistry, EPR, NMR, and FTIR spectroscopies and X-ray crystallography. It is found that NP1 readily binds NO in solution and in the crystalline state, but the protein is not readily autoreduced by excess NO. Likewise, dithionite is not a very effective reductant of NP1. However, the protein can be photoreduced by illumination with visible light in the presence of excess NO, deazaflavin, and EDTA. Optical spectra of the $Fe^{III}NO$ and $Fe^{II}NO$ complexes of NP1 are extremely similar, which makes it difficult to characterize the oxidation state of the NO complex by UV−visible spectroscopy. The reduction potential of NP1 in the absence of NO is ∼300 mV more negative than that of metmyoglobin (metMb). In the presence of NO, the reduction potential shifts ∼+430 mV for NP1−NO, but the reduction potential of metMb−NO cannot be measured for comparison. Based on estimated values of K_d for $NP1^{III}$−NO, the K_d values for the Fe^{II}−NO complex are 20.8 and 80.6 fM at pH 5.5 and 7.5, respectively. The lower driving force for NP1 reduction is qualitatively consistent with the slower rate of autoreduction of NP1−NO; the negative charges surrounding the heme probably also play a role in determining the much slower rate of autoreduction. The N−O stretching frequencies of $NP1^{III}$−NO and $NP1^{II}$−NO were measured by FTIR spectroscopy. The values obtained are very typical of other heme−NO stretching frequencies in the two oxidation states: ν_{NO} = 1917 and 1904 cm^{-1} for two species of $Fe^{III}NO$ and 1611 cm^{-1} for Fe^{II}-NO; the values of ν_{NO} are consistent with 6-coordinate "base-on" heme−NO centers for both oxidation states. The breadths of the IR bands are consistent with the large solvent accessibility of the bound NO of NP1 and also with the possibility of minor dissociation of the protein-provided histidine ligand on the IR time scale. The ratio of the two Fe^{III}−NO species changes with pH and the nature of the buffer. The CO complex of the Fe(II) form of NP1 has ν_{CO} = 1960 and 1936 cm^{-1}, again showing the presence of two species. Both NMR and X-ray crystallography show that the protohemin center of NP1 imidazole has a very high preference for a single orientation of the unsymmetrical protoheme moiety. The structure shows the Fe−N−O unit to be quite bent, which is consistent with its being the Fe^{II}−NO form of the protein, presumably formed by photoreduction in the X-ray beam. The proximal base, His-59, is clearly coordinated to the iron in the crystalline state and in solution at ambient temperatures, based on FTIR data, but EPR studies of dithionite-reduced samples show that a percentage of the protein has lost the histidine ligand from the $Fe^{II}NO$ center in frozen solution.

Introduction

Among the vast array of substances found in the saliva of blood-sucking arthropods that contribute to these insects' ability to obtain a sufficient blood meal are components that counteract blood coagulation, platelet function, and vasoconstriction.[1−4] Because insects from many different orders have evolved to feed on the blood of higher animals, convergent evolution is believed to be responsible for these organisms' development of a large variety of antihemostatic compounds.[5] Within the order *Hemiptera*, insects in two different families have been found to have salivary vasodilatory components that are NO-carrying heme proteins. The insects in question are a member of the kissing bug family, *Rhodnius prolixus*,[6,7] and the bedbug, *Cimex lectularius*.[8] Because of their ability to reversibly bind

[†] Department of Chemistry, University of Arizona.
[‡] Department of Biochemistry, University of Arizona.
[§] University of Amsterdam.
[||] Present address: Laboratorium fhr Mikrobiologie, Fachbereich Biologie, Philipps-Universität, Karl-von-Frisch-Strasse, D-35032 Marburg, Germany.

(1) Ribeiro, J. M. C. *Annu. Rev. Entomol.* **1987**, *32*, 463.
(2) Law, J.; Ribeiro, J. M. C.; Wells, M. A. *Annu. Rev. Biochem.* **1992**, *61*, 87.
(3) Ribeiro, J. M. C.; Garcia, E. S. *J. Exp. Biol.* **1981**, *94*, 219.
(4) Ribeiro, J. M. C.; Rossignol, P. A.; Spielman, A. *J. Exp. Biol.* **1984**, *108*, 1.
(5) Ribeiro, J. M. C.; Nussenzveig, R. H.; Tortorella, G. *J. Med. Entomol.* **1994**, *31*, 747.
(6) Ribeiro, J. M. C.; Gonzales, R.; Marinotti, O. *Br. J. Pharmacol.* **1990**, *101*, 932.
(7) Ribeiro, J. M. C.; Hazzard, J. M. H.; Nussenzveig, R. H.; Champagne, D. E.; Walker, F. A. *Science* **1993**, *260*, 539.

10.1021/ja982979i CCC: $18.00
Published on Web 12/17/1998

nitric oxide, this new class of heme proteins has been named nitrophorins, NP.[9] The small, gaseous NO molecule, released (both because of dilution and of pH elevation) upon injection of the nitrophorins into the tissue of the victim, can diffuse through tissue to the capillaries to cause vasodilation. The recent award of the 1998 Nobel Prize in medicine to Furchgott, Ignarro, and Murad for their discoveries concerning nitric oxide as a signaling molecule in the cardiovascular system points up the importance of understanding the chemistry of NO and ways in which it may be stabilized in biological systems. As we will show, the nitrophorins from *R. prolixus* are exquisitely designed for storage of NO in the insect saliva over long periods of time, perhaps up to a month.

Nitric oxide is unique among diatomic molecules in that it can bind to many metals of different oxidation states and different electron configurations. Some years ago, Enemark and Feltham developed the $\{MNO\}^n$ formalism to describe the number of metal d plus NO π^* electrons present in the MNO unit; they found that, for $n = 6$ or less, the MNO unit is linear, while for $n = 7$ and greater the MNO unit is bent.[10] In terms of model heme−NO complexes, both Fe^{III}−NO ($\{FeNO\}^6$) and Fe^{II}−NO ($\{FeNO\}^7$) complexes have been characterized spectroscopically and structurally.[11,12]

Recent studies of the nitrophorins of *R. prolixus* have included cloning and sequencing the gene for nitrophorin 1 (NP1)[9] (the most abundant of the four salivary nitrophorins), expressing, renaturing, and reconstituting the recombinant protein with hemin,[13] growing diffraction-quality crystals, and solving the structure of NP1 as the ammonia, cyanide, and histamine complexes.[14] As we showed earlier,[7] the NP1−NO complex is EPR silent because it contains an odd-electron (ferriheme) center bound to the odd-electron diatomic, NO, which creates a $\{FeNO\}^6$ center. The NMR spectrum of $NP1^{III}$−NO is that of a diamagnetic protein.[15] However, whether the electron configuration is best described as Fe^{II}−NO^+ or antiferromagnetically coupled low-spin Fe^{III}−$NO^\bullet$ is not completely clear, even from Mössbauer spectroscopic investigations of model heme−NO complexes currently in progress.[16] That this is a ferriheme protein helps to explain the fact that the NO dissociation constant is in the micromolar range,[13] rather than the picomolar range, as would be expected for a ferroheme−NO center.[17] Histamine has also been shown to bind to NP1[18] with a dissociation constant 50 times smaller than that for NO at pH 7,[13,14] suggesting that NP1 actually has two roles in ensuring that the insect obtains a sufficient blood meal: (i) releasing NO, which can rapidly diffuse through the tissue from the site of the bite to the nearby capillaries and cause vasodilation to bring more blood to the site of the wound (as well as to prevent platelet aggregation), and (ii) taking up histamine that is released by the victim in response to the bite, to temporarily reduce swelling and the onset of the immune response.[14] Indeed, the structure of the NP1−histamine complex shows excellent hydrogen-bonding patterns for all acidic protons of the coordinated, amino-protonated histamine molecule, as well as extensive van der Waals contacts between leucines 123 and 133 and both faces of the imidazole portion of the histamine molecule.[14]

We have attempted to determine the structure of the NO complex of NP1, but as reported below, our attempts have invariably met with apparent photoreduction of the protein from the physiologically active ferriheme−NO form to the inactive (with respect to release of NO) ferroheme−NO form in the X-ray beam. Ironically, photoreduction appears to be one of the best means of producing $NP1^{II}$−NO, as our IR studies presented in this work have demonstrated.

In the present work we describe our investigations of the redox chemistry of NP1 and its NO complex, its characterization by NMR, EPR, and FTIR spectroscopic techniques, and the structure of the reduced NP1−NO complex. We are continuing our attempts to understand the resistance to heme reduction in these proteins, which is necessary for NO storage and, especially, for NO release.

Numerous reports of the EPR spectra of ferroheme−NO centers have appeared, as reviewed recently.[19] Reports of the UV−visible and IR spectra of both ferro- and ferriheme−NO centers have also recently been reviewed.[19] In particular, the UV−visible spectra of the ferric and ferrous NO complexes of myoglobin have been reported by several authors,[20,21] but the similarity of both the wavelength maximums and extinction coefficients has not been appreciated by some later workers, leading some investigators to possibly mistakenly confuse one oxidation state with the other. In this work, we show that the optical spectra of the ferrous and ferric NO complexes of NP1 are similar enough that this spectroscopic technique is not reliable for differentiating the two oxidation states. Thus, as we show in this work, the change (or lack thereof) in optical spectra upon blowing argon over the sample, or recording the EPR spectrum of the sample, is the only way to quickly and reliably determine the oxidation state of the iron in the heme−NO center. EPR spectroscopy is also valuable for determining the presence of the Fe^{II}−NO center and coordination number of the iron, for the 5-coordinate (base off) FeNO EPR spectrum is quite different from that of the 6-coordinate (base on) FeNO species.[19]

Infrared spectra of various heme−NO systems have been reported, including a number of NO complexes of ferro- and ferriheme proteins.[22−25] As part of this work, we have characterized the ferro- and ferriheme−NO complexes of NP1 by FTIR spectroscopy.

Experimental Section

Electrochemical Measurements. Electrochemical reduction of NP1 (prepared as described previously[13]), horse heart metMb (Sigma), and their respective NO complexes was investigated by spectroelectro-

(8) Valenzuela, J. G.; Walker, F. A.; Ribeiro, J. M. C. *J. Exp. Med.* **1995**, *198*, 1519.
(9) Champagne, D. E.; Nussenzveig, R.; Ribeiro, J. M. C. *J. Biol. Chem.* **1995**, *270*, 8691.
(10) Feltham, R. D.; Enemark, J. H. *Coord. Chem. Rev.* **1974**, *13*, 339.
(11) (a) Piciulo, P. L.; Scheidt, W. R. *J. Am. Chem. Soc.* **1976**, *98*, 1913. (b) Scheidt, W. R.; Brinegar, A. C.; Ferro, E. B. Kirner, J. F. *J. Am. Chem. Soc.* **1977**, *99*, 7315.
(12) (a) Scheidt, W. R.; Lee, Y. J.; Hatano, K. *J. Am. Chem. Soc.* **1984**, *106*, 3191. (b)Ellison, M. K.; Scheidt, W. R. *J. Am. Chem. Soc.* **1997**, *119*, 7404. (c) Ellison, M. K.; Scheidt, W. R. Submitted for publication.
(13) Andersen, J. F.; Champagne, D. E.; Weichsel, A.; Ribeiro, J. M. C.; Balfour, C. A.; Dress, V.; Montfort, W. R. *Biochemistry* **1997**, *36*, 4423.
(14) Weichsel, A.; Andersen, J. F.; Champagne, D. E.; Walker, F. A.; Montfort, W. R. *Nature Struct. Biol.* **1998**, *5*, 304.
(15) Shokhireva, T. Kh. Unpublished results.
(16) Schhnemann, V.; Winkler, H.; Trautwein, A. X.; Walker, F. A. Manuscript in preparation.
(17) Traylor, T. G.; Sharma, V. S. *Biochemistry* **1992**, *31*, 2847.
(18) Ribeiro, J. M. C.; Walker, F. A. *J. Exp. Med.* **1994**, *180*, 2251.
(19) Walker, F. A.; Ribeiro, J. M. C.; Montfort, W. R. In *Metals in Biological Systems*; Sigel, H., Sigel, A., Eds.; Marcel Dekker: New York, 1998; Vol. 36, pp 619−661.
(20) Romberg, R. W.; Kassner, R. J. *Biochemistry* **1979**, *18*, 5387.
(21) Addison, A. W.; Stephanos, J. J. *Biochemistry* **1986**, *25*, 4104.
(22) (a) Maxwell, J. C.; Caughey, W. S. *Biochemistry* **1976**, *15*, 388. (b) Sampath, V.; Zhao, X.-J.; Caughey, W. S. *Biochem. Biophys. Res. Commun.* **1994**, *198*, 281. (c) Zhao, X. J.; Sampath, V.; Caughey, W. S. *Biochem. Biophys. Res. Commun.* **1994**, *204*, 537.
(23) Miller, L. M.; Pedraza, A. J.; Chance, M. R. *Biochemistry* **1997**, *36*, 6, 12199.
(24) Wang, Y.; Averill, B. A. *J. Am. Chem. Soc.* **1996**, *118*, 3972.
(25) Obayashi, E.; Tsukamoto, K.; Adachi, S.; Takahashi, S.; Nomura, M.; Iizuka, T.; Shoun, H.; Shiro, Y. *J. Am. Chem. Soc.* **1997**, *119*, 7807.

chemical techniques[26] using a BAS CV-50W voltammetric analyzer and a Spectral Instruments spectrophotometer or a Cary 14 spectrophotometer modified by On-Line Instrument Systems, Inc., all under computer control. The optically transparent thin-layer working and counter electrodes (OTTLE) were gold minigrid, 200 wires/in., 70% transmittance, purchased from Buckbee Mears. The reference electrode was a Ag/AgCl electrode (BAS). The OTTLE cells were of the design of Balfe,[27] modified from the original designs of Hawkridge[28] and Heineman,[29] and were assembled according to procedures described previously.[26c,30] Solutions of each of the proteins (~0.05 mM) plus 1 mM methyl viologen (Aldrich) ($E^{\circ\prime} = -447$ mV vs NHE[31]) and 0.2 mM $Ru(NH_3)_6Cl_3$ (Alfa) ($E^{\circ\prime} = +51$ mV vs NHE[32]) were prepared in ~0.1 M ionic strength phosphate buffer at pH 7.5, 6.5, and 5.5. Each solution was degassed several times by application of a vacuum followed by introduction of argon. Each sample was then introduced into the OTTLE cell under argon and prepared for potentiometric titration. Fully oxidized spectra were obtained at an applied potential of 0 mV vs Ag/AgCl (+205 mV vs NHE), while fully reduced spectra were obtained at an applied potential of −600 mV vs Ag/AgCl (NP1) or −400 mV (Mb). For each sample, the potential was stepped from −530 to −410 mV (NP1) or −240 to −120 mV (Mb) vs Ag/AgCl in 10-mV steps. Optical spectra were recorded over the range 350−500 nm after the sample had reached equilibrium following each step in applied potential (typically 10 min). The temperature in the sample chamber was 28 ± 1 °C.

For NO-containing samples, NO was blown over the solution for 10 min, followed by argon for several minutes; each sample was then introduced into the OTTLE cell under argon. Fully oxidized spectra were obtained without applied potential for NP1−NO; it was not possible to obtain the spectra of fully oxidized Mb−NO because of facile dissociation of NO. Fully reduced spectra were obtained at an applied potential of −400 mV vs Ag/AgCl (NP1−NO and Mb−NO). For each sample, the potential was stepped from −160 to −70 mV (NP1−NO) vs Ag/AgCl in 10-mV steps. Optical spectra were recorded over the wavelength range 350 to 650 nm. The cell temperature was 27 ± 1 °C.

EPR Spectroscopy. EPR spectra were acquired using a Bruker ESP 300 E spectrometer operating at 9.38 GHz with 200 μW of microwave power. The modulation frequency was 100 kHz, and the modulation amplitude was 2 G. The spectra were acquired at 4.2 K using the model ESR 900 Oxford Instruments cryostat. EPR samples of $NP1^{II}$−NO were prepared in 30 mM phosphate buffer at pH 7.0 and 30 mM acetate buffer at pH 5.0. Samples were degassed under argon in a glovebag and prereduced with crystals of dithionite. NO was then blown over the samples for 5 min, which were then transferred to quartz EPR tubes (Wilmad), capped, and immediately frozen in liquid nitrogen, where they were stored until EPR spectra were recorded.

NMR Spectroscopy. One-dimensional proton NMR spectra were acquired on the imidazole complex of NP1 on a Bruker AM 500 spectrometer operating in quadrature detection mode. The 6 mM NP1 sample in D_2O (Cambridge Isotope Laboratories) containing 30 mM phosphate buffer at pH 7.0 (uncorrected for the deuterium isotope effect) was carefully titrated with imidazole (Aldrich) until the high-spin ferriheme signals in the 40−70 ppm region disappeared and were replaced by the low-spin ferriheme signals in the 12−28 ppm region. Spectra were obtained at 30 °C immediately after dissolution of the lyophilized NP1 sample and titration with imidazole and then again 12 h later.

FTIR Spectroscopy. Desalted lyophilized recombinant ferric NP1 was dissolved in water and concentrated with Minicon PM10 ultrafiltration devices (8000*g*) to concentrations of 3−15 mM. Minor precipitates were removed by centrifugation for 10 min at 14000*g* at room temperature. Buffer components, deazaflavin, or sodium dithionite were added as concentrated stock solutions. In control experiments, it was shown that the pH of the resulting solutions did not deviate more than 0.1 unit from the original stock. Samples of typically 10−15 μL were put in 500-μL Eppendorf vials of which the top had been cut off. These were carefully inserted into an 8-mL Subasealed glass vial. For preparation of the CO and NO derivatives and the photoreduction, the vials were made anaerobic by six vacuum−argon cycles (the argon was passed through an Oxisorb cartridge, Messer-Griesheim, Düsseldorf, Germany). Residual oxygen was allowed to diffuse out of the liquid for 15 min, after which an additional series of vacuum−argon cycles was applied. The CO derivative was prepared by addition of freshly prepared anaerobic sodium dithionite stock solution in the identical buffer, incubation for 5 min, and purging with 99.99% CO gas for 5 min. The NO derivatives were made by in situ generation of NO from 10 mg of solid $NaNO_2$ and 1 mL of anaerobic 0.2 M KI/0.4 M H_2SO_4 (in D_2O for the deuterated solutions). To release the overpressure, a thin needle was briefly inserted into the Subaseal. $Na^{15}NO_2$ (enrichment >98%, technical grade, was obtained from Cambridge Isotope Laboratories). To equilibrate the NP1 with the gaseous headspace, a tightly fitting 50-μL Hamilton syringe was pulled up and down vigorously 5 min to get some gas bubbles into the liquid. The same Hamilton syringe was used to transfer the samples to a homemade IR transmittance cell, composed of a sandwich of polished CaF_2 plates (3-mm thickness) and a Teflon spacer (56 μm) or a polyethylene bag obtained from a local supermarket (13 μm). The IR cell was purged with argon before loading. Manipulations were performed at room temperature and in dim light. Photoreduction was carried out by irradiation of buffered samples containing 1 mM deazaflavin, 50 mM EDTA, and 50 mM Tris-HCl at pH 8 for 30 min with an Oriel 150-W xenon arc source focused via a quartz optical fiber. The optical path contained a heat filter.

FTIR measurements were performed at room temperature on a Bio-Rad FTS 60A spectrometer equipped with an MCT detector and a KBr beam splitter. Absolute absorbance spectra were recorded using buffer or single-beam spectra. For the photoreduction experiments, the difference spectrum was recorded using the single-beam spectrum before photoreduction of sample as reference. The FTIR spectrometer was purged with dry pressurized air for at least 30 min after insertion of the samples to minimize water vapor bands. Corrections for absorption by solvent, protein, and water vapor were performed with the software supplied by Bio-Rad. After these corrections, the multiple-point baseline method was used to obtained a flat baseline in the region where no NO or CO absorption is expected (Figure 6 below). This was not necessary for Figure 7 (see below). Simulation of the infrared (difference) spectra was performed with EXCEL 6.0 using the solver macro and a least-squares fit of experimental vs simulated spectrum in the range of interest. Routinely UV−visible spectra were recorded of the infrared samples with an HP-8452A diode array spectrophotometer equipped with a homemade sample holder for infrared samples. The extinction coefficients used were 169 mM^{-1} cm^{-1} at 406 nm for ferric, 12.5 mM^{-1} cm^{-1} at 550 nm for ferrous CO, and 31 mM^{-1} cm^{-1} for ferric NO at 340 nm. The extent of reduction was determined from the disappearance of the ferric−NO band in the infrared spectrum (vide infra).

X-ray Crystallography. NP1 concentrated by ultrafiltration in a Centricon-10 filter was crystallized by the hanging drop method in 2.8 M ammonium phosphate/0.1 M cacodylate buffer at pH 7.2. The cherry red platelike crystals probably had ammonia bound to the heme iron, as previously described.[14] To remove ammonia from the heme-binding site, the crystals were washed in several solutions with decreasing concentrations of ammonium phosphate and increasing concentrations of potassium phosphate. During that procedure, a gradual change in the crystal color from cherry red to dull green-brown was noticed. The crystals were equilibrated for 1 h in 3.2 M potassium phosphate/0.1 M

(26) (a) Hawkridge, F. M.; Kuwana, T. *Anal. Chem.* **1973**, *45*, 1021. (b) Crutchley, R. J.; Ellis, Jr.; W. R.; Gray, H. B. *J. Am. Chem. Soc.* **1985**, *107*, 5002. (c) Walker, F. A.; Emrick, D.; Rivera, J. E.; Hanquet, B. J.; Buttlaire, D. H. *J. Am. Chem. Soc.* **1988**, *110*, 6234. (d) Hildebrand, D. P.; Tang, H.; Luo, Y.; Hunter, C. L.; Smith, M.; Brayer, G. D.; Mauk, A. G. *J. Am. Chem. Soc.* **1996**, *118*, 12909.

(27) Balfe, C. A. Ph.D. Dissertation, University of California, Berkeley, 1984.

(28) Bowen, E. F.; Hawkridge, F. M. *J. Electroanal. Chem. Interfacial Electrochem.* **1981**, *125*, 367.

(29) Norris, B. J.; Meckstroth, M. L.; Heineman, W. R. *Anal. Chem.* **1976**, *48*, 630.

(30) Emrick, D. M.S. Thesis, San Francisco State University, 1986.

(31) Hawkridge, F. M.; Kuwana, T. *Anal. Chem.* **1973**, *45*, 1021.

(32) (a) Lim, S. M.; Barclay, D. J.; Anson, F. C. *Inorg. Chem.* **1972**, *11*, 1460. (b) Ried, L. A.; Taniguchi, V. T.; Gray, H. B.; Mauk, A. G. *J. Am. Chem. Soc.* **1982**, *104*, 7516.

Table 1. Crystallographic Data

crystal system	monoclinic
space group	$P2_1$
a, Å	39.4
b, Å	74.3
c, Å	66.1
β, deg	99.2
Z	4
resolution, Å	2.3
no. of observed reflections	29574
no. of unique reflections	18013
completeness, %	93.5
R_{sym}[a]	0.052
R_{cryst}[b]	0.19
R_{free}[c]	0.29
rmsd bonds, Å	0.013
rmsd angles, deg	1.8

[a] $R_{sym} = (\sum_h|I_h - \langle I\rangle|)/(\sum_h I_h)$, where $\langle I\rangle$ is the mean intensity of all symmetry-related reflections I_h. [b] $R_{cryst} = (\sum|F_{obs} - F_{calc}|)/(\sum F_{obs})$. [c] R_{free} as for R_{cryst} using a random subset of the data (5%) not included in the refinement.

potassium cacodylate, pH 6.8, and the solution was placed into a sealed tube and purged with argon for 3 h to remove oxygen. The tube was then placed in a glovebag, and the crystals were transferred under argon atmosphere into an identical buffered solution saturated with NO to a ~2 mM concentration. Formation of the NP1−NO complex was indicated by a change in color from dull green-brown to cherry red. A single 0.7 × 0.4 × 0.1 mm crystal of the complex was mounted in a glass capillary under argon atmosphere in a glovebag.

Diffraction data were measured using a Cu X-ray source with a graphite monochromator and an Enraf Nonius FAST area detector and reduced with programs MADNES,[33] PROCOR,[34] and CCP4.[35] The structure was refined with X-PLOR[36] starting with a model of the NP1−NH_3 complex (PDB entry 2NP1), which was isomorphous with the NP1−NO crystals.[14] Manual rebuilding with FRODO[37] and O,[38] positional refinement with bulk solvent correction, and individual temperature factor refinement to 2.3 Å resulted in a final model, which was deposited in the PDB with accession number 4NP1. The crystallographic data are summarized in Table 1.

Results

UV−Visible Spectra. Optical spectra of the ferric and ferrous NP1−NO complexes at pH 5.5 as a function of applied potential are shown in Figure 1. The protein concentration in this and the other spectroelectrochemical experiments described below was ~0.05 mM (see Experimental Section), well above the $NP1^{III}$−NO dissociation constant for all pH values studied (0.35−1.35 μM).[13] As is evident, good isosbestic behavior is observed. The spectral changes were reversible over many cycles of positive and negative applied potential, as positive as +600 mV vs Ag/AgCl (+805 mV vs NHE). The ferric form of NP1−NO has the higher extinction coefficients and sharper Soret and α,β bands, the situation usually observed for a diamagnetic Fe(II) heme center. There is only a 3-nm shift in the position of the Soret band upon reduction of $NP1^{III}$−NO to $NP1^{II}$−NO− from 419 to 416 nm; these Soret band positions do not change over the pH 5.5−7.5 range. In comparison, using acetate buffer at pH 5, it was previously shown that the Soret band maximum of $NP1^{III}$−NO shifts from 419 (pH 7) to 421 nm (pH 5).[13]

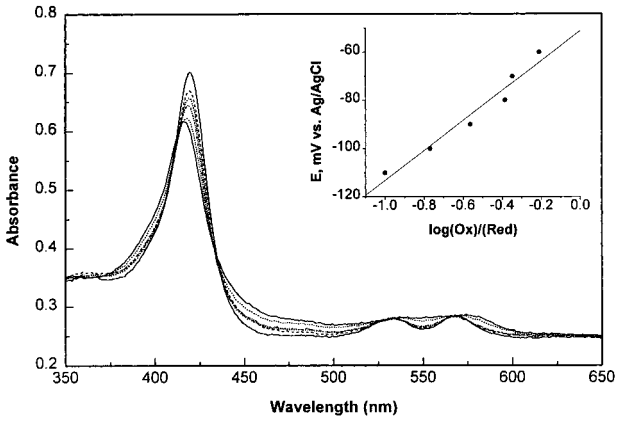

Figure 1. UV−visible spectra of NP1−NO at pH 5.5 as a function of applied potential. In order of decreasing Soret band heights: no applied potential, +200, −40, −60, −100, and −400 mV vs Ag/AgCl, respectively (add 205 mV for potential vs NHE). Inset: Nernst plot of the spectroelectrochemical data.

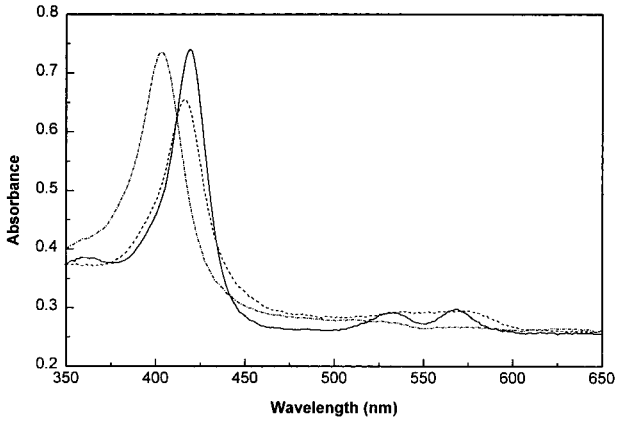

Figure 2. UV−visible spectra of NP1−NO at pH 7.5 as a function of applied potential. Solid line, no applied potential; dashed line, −400 mV vs Ag/AgCl; dotted line, +600 mV vs Ag/AgCl.

At pH 7.5, the spectral changes of NP1−NO upon potentiometric titration are quite different from those observed at pH 5.5. (These pH values were chosen because they represent the probable extremes in pH experienced by the protein in vivo: The pH of animal tissues is somewhat above 7, while that of insect saliva is considerably lower.) While the NO complex at pH 7.5 shows a Soret band maximum of 419 nm in the absence of applied potential and of 416 nm in the presence of a reducing potential of −400 mV vs Ag/AgCl (−195 mV vs NHE), application of a positive potential of up to +600 mV vs Ag/AgCl (+805 mV vs NHE) caused the Soret band to shift to 403 nm (Figure 2), indicating that the oxidized form, $NP1^{III}$−NO, readily loses NO when a potential positive enough to oxidize NO[39] is applied (see also Figure 3, discussed below, for the UV−visible spectrum of NP1 in the absence of NO). These changes were reversible over many cycles of positive and negative applied potential. Spectral shifts could be induced either by increasing the potential from 0 to +600 mV vs Ag/AgCl in a stepwise fashion or by raising the potential immediately from 0 to +600 mV and then recording the spectrum as a function of time (over the period of 0.5 h).

In comparison to the spectra of the nitric oxide complexes, the optical spectra of the ferric and ferrous forms of NP1 in the

(33) Messerschmidt, A.; Pflugrath, J. W. *J. Appl. Crystallogr.* **1987**, *20*, 306.
(34) Kabsch, W. *J. Appl. Crystallogr.* **1988**, *21*, 916.
(35) Collaborative Computational Project, No. 4. *Acta Crystallogr.* **1994**, *D50*, 760.
(36) Brunger, A. T.; Kuriyan, J.; Karplus, M. *Science* **1987**, *235*, 458.
(37) (a) Jones, A. *J. Appl. Crystallogr.* **1978**, *11*, 268. (b) Pflugrath, J. W.; Saper, M. A.; Quiocho, F. A. In *Methods and Applications in Crystallographic Computing*; Hall, S., Ashida, T., Eds; Clarendon Press: Oxford, 1984; pp 404−407.
(38) Jones, T. A.; Zou, J. Y.; Cowan, S. W.; Kjelgard, M. *Acta Crystallogr.* **1991**, *A47*, 110.

(39) We find that NO is reversibly oxidized to NO_2^- at a potential of +600 mV vs NHE.[40]

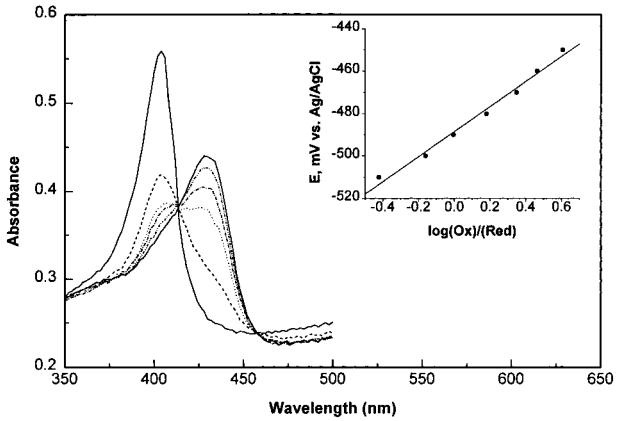

Figure 3. UV−visible spectra of NP1 in the absence of NO at pH 6.5 as a function of applied potential. Solid line, fully oxidized NP1, λ_{max} = 403 nm; dash−dotted line, fully reduced NP1, λ_{max} = 430 nm.

absence of NO over the pH range of 5.5−7.5 show the more typically expected changes in Soret band maximum (Figure 3): The high-spin $NP1^{III}$ species has its Soret band maximum at 403 nm, while the high-spin $NP1^{II}$ has its Soret band maximum at 430 nm at pH 5.5. In both cases, the α,β bands are quite broad and of low extinction (not shown).

In comparison to NP1, horse heart metmyoglobin (metMb) showed similar spectral changes upon reduction in the absence of NO, but in the presence of NO at pH 7.5 and 6.5, there appeared to be much less difference in the optical spectra in the absence of an applied potential or with an applied potential of −400 mV vs Ag/AgCl. The Soret band shifted only 1 nm upon application of the reducing potential (420 to 421 nm), and the extinction coefficient changed only imperceptibly. Hence, the optical spectra of Mb^{III}−NO and Mb^{II}−NO are extremely similar, as reported previously by Addison and Stephanos.[21] In contrast, in the presence of a more positive potential (−50 mV vs Ag/AgCl), the Soret band shifted back to 410 nm, indicating that NO had dissociated when the complex was maintained in the fully oxidized Fe(III) form, with an applied potential much lower than that of the NO/NO_2^- oxidation potential. At pH 5.5, in the absence of an applied potential, the Soret band was broadened over the entire 350−420-nm range, suggesting some modification of the heme π electronic system at this pH in the absence of an applied potential (or with an applied potential of 0 mV vs Ag/AgCl). However, application of a negative potential (−400 mV vs Ag/AgCl) restored the Soret band of the reduced Mb−NO complex (λ_{max} = 421 nm).

Electrochemical Results. Using the spectral data of Figures 1 and 3, and similar data obtained for myoglobin in the absence of NO, Nernst plots such as those shown in the insets of Figures 1 and 3 were constructed and the midpoint potentials of NP1, Mb, and NP1−NO were calculated. The results are summarized in Table 2, where all potentials are expressed vs NHE (+205 mV with respect to the Ag/AgCl reference electrode used for the spectroelectrochemical measurements). It can be seen that the reduction potential of NP1 in the absence of NO is ∼300 mV more negative than that of Mb in the absence of NO, and the reduction potential of NP1−NO is ∼430 mV more positive than that of NP1 in the absence of NO. Nevertheless, when the potentiostat is turned off, fully reduced samples of $NP1^{II}$−NO (which contain no excess NO) are observed to slowly revert (autoxidize) to $NP1^{III}$−NO. The nature of the oxidant is unknown. It was not possible to measure the reduction potential of Mb−NO at any pH in the 5.5−7.5 range because of facile dissociation of NO from the Fe(III) form of the protein in the absence of excess NO, as well as the small change in Soret band maximum and extinction coefficient of the NO complexes of the two oxidation states.

Table 2. Reduction Potentials of NP1, metMb, and NP1−NO as a Function of pH[a]

protein	pH	*T*, °C (±1 °C)	$E^{o\prime}$ (mV vs NHE)	slope of Nernst plot (mV)
Mb	5.5	28	+28 ± 1	61 ± 1
	6.5	28	+12 ± 2	59 ± 1
	7.5	28	0 ± 2	61 ± 1
NP1	5.5	28	−274 ± 1	60 ± 1
	6.5	28	−284 ± 2	59 ± 3
	7.5	28	−303 ± 4	60 ± 2
NP1−NO	5.5	27	+154 ± 5	62 ± 7
	7.5	27	+127 ± 4	61 ± 11

[a] Ionic strength ∼0.1 M.

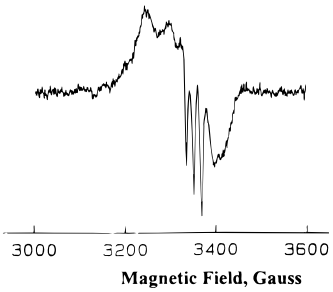

Figure 4. EPR spectrum of $NP1^{II}$−NO in 30 mM acetate buffer, pH 5.0, recorded at 4.2 K at X-band. The signal is a combination of those characteristic of 5- and 6-coordinate $Fe^{II}NO$ heme centers.[39,40]

EPR Spectra. Figure 4 shows the EPR spectrum of a sample of $NP1^{II}$−NO at pH 5.0. As is apparent, both 5- and 6-coordinate Fe^{II}−NO species[41,42] are present. This suggests that the protein tends to lose its proximal histidine upon reduction by dithionite, although in the crystalline state, the His-59 bond to the heme iron is intact, as discussed below.

NMR Spectra. The ^1H hyperfine shifted resonances of the imidazole complex of NP1 for freshly dissolved lyophilized protein vs protein equilibrated in buffered D_2O for 12 h are shown in Figure 5. A number of heme resonances seen shortly after dissolving the sample and adding imidazole disappear after equilibration, indicating that, unlike many other noncovalently bound *b* heme-containing proteins such as cytochromes b_5,[43] one orientation of the unsymmetrical heme group is so strongly favored that there is no evidence of the other heme orientation in the NMR spectrum of the 12-h-equilibrated sample. This result is consistent with the crystallographic findings for the NH_3, cyanide, and histamine complexes,[14] as well as for the NO complex of the reduced protein discussed below, where in each case the heme appears to be in only one orientation (i.e., that the electron density of the vinyl groups is in each case well described with only one heme orientation). A single orientation is also found in the 1.5-Å resolution crystal structure of NP4, which has 90% sequence identity with NP1.[44]

FTIR Spectra. Representative FTIR spectra of the ferrous and ferric NP1−NO and ferrous NP1−CO complexes are shown in Figure 6, and $^{14}NO/^{15}NO$ difference spectra of the ferrous

(40) Wehle, D. M.S. Thesis, University of Arizona, 1998.
(41) Yoshimura, T. *J. Inorg. Biochem.* **1983**, *18*, 263.
(42) Brunori, M.; Falcioni, G.; Rotilio, G. *Proc. Natl. Acad. Sci. U.S.A.* **1974**, *71*, 2470.
(43) (a) La Mar, G. N.; Burns, P. D.; Jackson, J. T.; Smith, K. M.; Langry, K. C.; Strittmatter, P. *J. Biol. Chem.* **1981**, *256*, 6075. (b) Walker, F. A.; Emrick, D.; Rivera, J. E.; Hanquet, B. J.; Buttlaire, D. H. *J. Am. Chem. Soc.* **1988**, *110*, 6234.
(44) Andersen, J. F.; Weichsel, A.; Balfour, C.; Champagne, D. E.; Montfort, W. R. *Structure* **1998**, *6*, 1315.

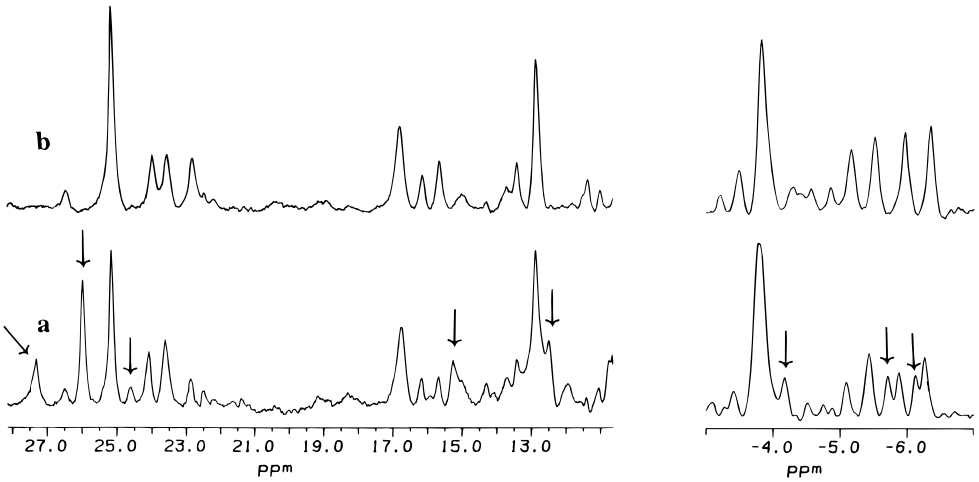

Figure 5. NMR spectra of NP1−imidazole (a) immediately after dissolution of lyophilized protein in D_2O buffered at pH 7.0 and (b) the same sample after 12 h. Resonances that decrease in intensity as a function of time are marked with arrows.

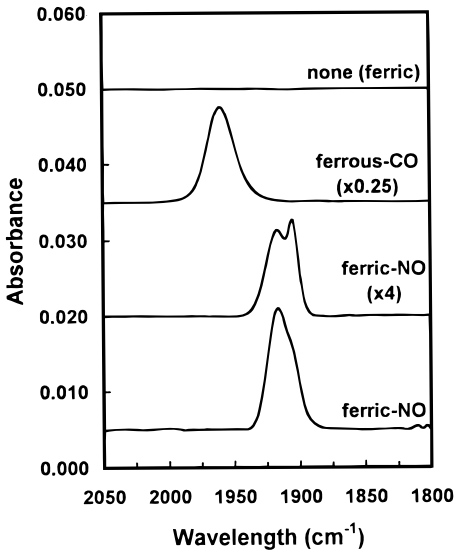

Figure 6. FTIR spectra of recombinant *R. prolixus* NP1. (a) Ferric NP1 (3.0 mM) exchanged into D_2O (50 mM citrate/NaOD, measured pH 5.6), path length 13 μm. (b) Ferrous CO derivative of NP1 (6.7 mM) in 50 mM Tris, 50 mM EDTA, 5 mM $Na_2S_2O_4$ pH 8, path length 56 μm (>90% CO complex). (c) Ferric NO derivative of NP1 (3.0 mM) in buffer identical to that for (a), path length 13 μm (73% NO complex). (d) Ferric NO derivative of NP1 (11.0 mM) in buffer identical to that for (b) with 1 mM deazaflavin rather than 5 mM $Na_2S_2O_4$, but not illuminated. The path length of the IR cell was 13 μm (95% NO complex). For the two ferrous−CO bands, the band positions are at 1960.3 and 1936 cm^{-1}, with line widths of 23.3 cm^{-1} and integral of 37 mM^{-1} cm^{-1}, very similar to other heme−CO complexes.[59] All spectra were recorded at a resolution of 2 cm^{-1} and are averages of 800 scans.

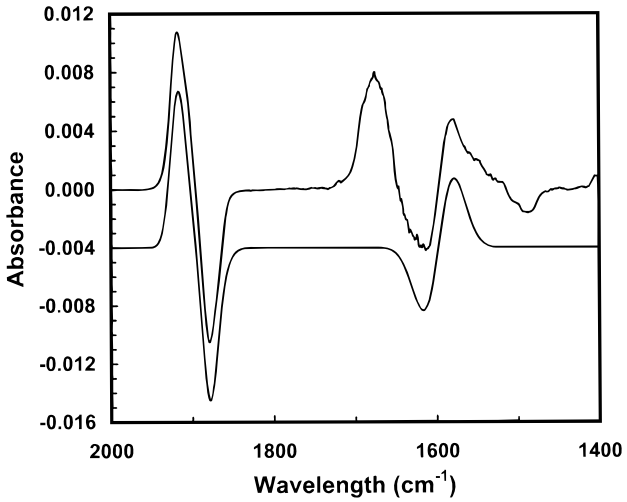

Figure 7. FTIR spectrum showing the (^{14}NO − ^{15}NO) isotope edited ferrous and ferric difference spectra of NP1−NO and a simulation thereof. The experimental spectrum was obtained by subtraction of the difference spectra (Fe(III) − Fe(II)) obtained upon photoreduction of natural-abundance NO ferric NP1 (11.0 mM, 95% NO complex, 35% reduction) and ^{15}NO ferric NP1 (9.2 mM, >97% NO complex, 76% reduction). The samples were in 50 mM Tris, 50 mM EDTA, 1 mM deazaflavin at pH 8 and were illuminated with a Xenon arc lamp to effect the photoreduction, as described in the Experimental Section. To correct for different degrees of reduction, extent of formation of NO derivatives, and protein concentration, the natural-abundance difference spectrum was multiplied by 1.88. Spectra were recorded at a resolution of 2 cm^{-1} and are averages of 800 scans. The FTIR spectrum was simulated using Gaussian-shaped curves with the following parameters (position, bandwidth, first integral, in cm^{-1}, cm^{-1}, and abs cm^{-1}, respectively): ^{14}NO ferric A, 1917.1, 21.2, 0.240, ^{14}NO ferric B, 1904.1, 9.1, 0.0242; ^{15}NO ferric A, 1879.5, 21.2, 0.225; ^{15}NO ferric B, 1866.9, 9.1, 0.0253; ^{14}NO ferrous, 1611.2, 40, 0.233; ^{15}NO ferrous, 1583.2, 40, 0.247. The quality of the fit of the ferrous bands is lower because of high background absorbance of the solvent and protein. For the ferrous complex, the best fit to the data depicted represents the solution with a separation of 28 cm^{-1} (and a bandwidth of 40 cm^{-1}) as has been observed in the ferrous−NO derivative of hemoglobin.[24]

and ferric forms are shown in Figure 7. In both cases, the isotope shifts are as expected. The data obtained for the ferrous and ferric NP1−NO complexes, along with those for other heme proteins and model complexes, are summarized in Table 3. As is evident from comparison to literature data, the ν_{NO} value of the ferrous NP1−NO complex is consistent with the base-on, hexacoordinate heme−NO complex and that of the ferric NP1−NO is similar to those of other Fe^{III}−NO hexacoordinate complexes. Two N−O stretching bands were observed for the Fe^{III}−NO samples, whose relative intensities varied with pH and nature of the buffer (Figure 6).

Ferrous NP1−NO Structure. The NP1−NO crystals are composed of two protein molecules in the asymmetric part of the unit cell (molecule I and molecule II) and are isomorphous with the other NP1 crystals so far examined.[14] The two crystallographically independent NP1 molecules have similar geometry, except that molecule I has a better defined loop for residues 32−38, which is disordered in molecule II. Figure 8 presents the structure of the NP1−NO complex, and Figure 9

Table 3. Summary of Infrared Data for Model Heme− and Heme Protein−NO Complexes, Including Nitrophorin 1

compound	frequency (cm^{-1}) ^{14}NO	frequency (cm^{-1}) ^{15}NO	$^{14}NO(^{15}NO)$ LWHM (cm^{-1})	integrated intensity (mM^{-1} cm^{-2})	ref
Ferrous−NO Complexes (Pentacoordinated)					
(octaethylporphyrinato)iron(II) (KBr)	1673				12b
(octaethylporphyrinato)iron(II) ($CHCl_3$)	1665				12b
protoheme dimethyl ester (KBr)	1660				22a
protoheme dimethyl ester (CCl_4)	1684		20		22a
protoheme dimethyl ester ($CHCl_3$)	1676		18		22a
protoheme dimethyl ester ($ClCH_2CH_2Cl$)	1669		28		22a
Human hemoglobin A inositol hexaphosphate complex	1668	1635	10		22a
Ferrous−NO Complexes (Hexacoordinated)					
protoheme dimethyl ester pyridine complex	1633		20		22a
protoheme dimethyl ester 1-methylimidazole complex	1618		24		22a
human hemoglobin A	1615	1587	10	25	22a
human hemoglobin A inositol hexaphosphate complex	1615	1587	10		22a
human hemoglobin A	1616	1588.1	8.9 (9.9)	13.8 (16.2)	22b
bovine heart cytochrome *c* oxidase (a_3)	1610.2	1581.5	6.3 (7.0)	15.2 (13.6)	22c
bovine heart myoglobin	1611.8	1580.4	10.2 (7.9)	11.2 (18.0[a])	22c
second species	1587.3		(5.6)		22c
human hemoglobin	1615	1587	10 (10)	24.6 (23.3)	24
horse skeletal muscle myoglobin	1613	1587	9 (8)		23
second species	1607	1582	(8[b])		23
nitrophorin 1 from *Rhodnius prolixus*	1611	1583	40 (40)[c]	(28)[d]	tw[e]
Ferric−NO Complexes (Pentacoordinated)					
(octaethylporphyrinato)iron(III) (KBr)	1862				12a
Ferric−NO Complexes (Hexacoordinated)					
$[Fe(OEP)(NMeIm)(NO)]^+$ (Nujol mull)	1912				12c
$[Fe(OEP)(NMeIm)(NO)]^+$ (KBr, two crystalline forms)	1890, 1920				12c
horseradish peroxidase		1865			22a
human hemoglobin A	1925		9		22b
cd1 nitrite reductase from *Pseudomonas stutzeri*	1910	1874	6.5 (6.5)		24
human hemoglobin A	1925	1889	8 (8)	11.6 (14.1)	24
nitric oxide reductase from *Fusarium oxysporum*	1851	1820	26 (26)		23
$P450_{cam}$ from *Pseudomonas putida,* substrate free	1806	1775	22 (22)		25
$P450_{cam}$ from *P. putida*, norcamphor complex	1818				25
$P450_{cam}$ from *P. putida*, adamantanone complex	1818				25
chloroperoxidase from *Caldariomyces fumago*	1868				25
horse skeletal muscle myoglobin	1927		9		23
horse skeletal muscle myoglobin H64L	1904		12		23
nitrophorin 1 from *R. prolixus*	1917	1879.5	21 (21)	28[f]	tw[e]
second species	1904	1867	9 (9)	28[f]	tw[e]

[a] The ferrous−^{15}N−^{16}O exhibits two bands; the integrated intensity listed is the sum of both species. [b] Band too weak to determine LWHM. [c] Not accurate; correlated with peak separation. See Figure 7 caption. [d] ^{14}NO not accurately determined; ^{15}NO similar to ferric form. [e] tw, this work. [f] Corresponds to the sum of the two species. Within experimental error, the integrated intensities of spectra exhibiting two bands (next to bottom trace in Figure 6) and those consisting mainly of one band (Figure 6, bottom trace, and Figure 7) were identical.

shows the arrangement of protein side chains in the immediate vicinity of the heme−NO center. The protein molecule has a unique structure for a heme protein, but one that is typical for a lipocalin,[44,45] with an eight-stranded antiparallel β barrel, and three α helices flanking the barrel. The structure is essentially identical with the NP1−CN structure,[14] apart from the Fe−N−O angle, which refined to 123° in molecule I (which had the more reliable ligand electron density) and to 135° in molecule II. The reason for this difference in the two angles most likely has to do with the photoreduction that appears to have occurred during data collection and the consequent shifting of the NO from linear to bent. Because this was occurring while data were being measured, less reliable electron density for the NO was obtained, which resulted in a bond angle that is only approximate. However, the NO is clearly extremely bent, on average with an Fe−N−O angle of 130°. The heme molecule with NO bound to the iron atom is located inside the β barrel and bound to His-59 on the proximal side of the heme. While the electron density for both the heme iron and His-59 are quite good, we cannot rule out the possibility that a small percent of the molecules in the crystal have His-59 dissociated from the heme, as was indicated by the frozen solution EPR spectral experiments described above. Only the propionate groups of the heme are solvent exposed, while the rest of the heme group is buried in the heme pocket. However, the NO moiety is exposed enough to the solvent to permit access by at least one water molecule. The protoporphyrin ring has a distinct buckle similar to that observed in other NP1 complexes,[14] though the iron and nitrogen atoms appear to be coplanar. There are no indications that NO reacted with NP1 at any other site than the heme.

Discussion

The UV−visible spectra of NP1−NO in its oxidized and reduced forms (Figure 1) are qualitatively similar to those of metMb−NO and Mb−NO. Our own optical spectra of the latter two are not shown in figures due to their extreme similarity to those reported previously.[20−22] For NP1−NO in its oxidized and reduced forms, the Soret bands are at 419 and 416 nm, respectively, while for metMb−NO and Mb−NO we find the

(45) (a) Flower, D. R. *Biochem. J.* **1996**, *318*, 1. (b) Newcomer, M. E., Jones, T. A.; Cqvist, J.; Sundelin, J.; Ericksson, U.; Rask, L.; Peterson, P. A. *EMBO J.* **1984**, 3, 1451. (c) Holden, H. M.; Rypniewski, W. R.; Law, J. H.; Rayment, I. *EMBO J.* **1987**, *6*, 1565. (d) Huber, R.; Schneider, M.; Mayr, I.; Muller, R.; Deutzmann, R.; Suter, F.; Zuber, H.; Falk, H.; Kayser, H. *J. Mol. Biol.* **1987**, *198*, 499.

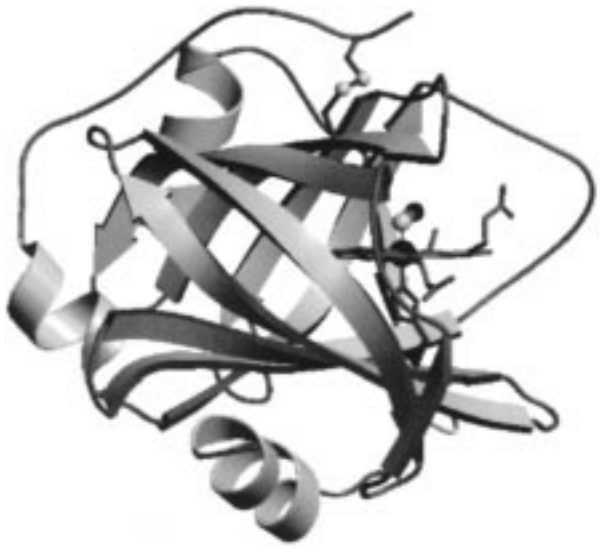

Figure 8. Structure of NP1−NO, showing the β-barrel lipocalin fold with the heme near the mouth of the barrel. The protein backbone is shown as a ribbon, disulfide bonds and NO as ball and sticks, and heme and His-59 as sticks. Note the bent NO unit, which identifies this as the structure of the reduced (Fe^{II}−NO) form of the protein.[11,12] Drawn with the programs MOLSCRIPT[71] and RASTER-3D.[72,73]

Soret bands are at 420 and 421 nm, respectively. Literature values for the latter two compounds are 420.5 and 421.5 nm at room temperature[20] and 420 and 422 nm at 5−25 K.[23] The larger difference in Soret band positions and extinction coefficients for oxidized and reduced NP1−NO than for the corresponding myoglobin complexes, plus the stability of the oxidized form of NP1−NO, have made it possible to measure the reduction potential of the NO complex of NP1 over the pH 5.5−7.5 range, while it was not possible to measure the reduction potential of the NO complex of metmyoglobin at any pH. Clearly, at extremely low temperatures, such as those used by the Chance group,[23] the metMb−NO complex is stable, while at room temperature, NO readily dissociates from metMb in the absence of a high concentration of free NO.

As is evident from Figure 1, good isosbestic behavior is observed for the NP1−NO complexes. The ferric form of NP1−NO has the higher extinction coefficients and sharper Soret and α,β bands, the situation usually reserved for a diamagnetic Fe(II) heme center. This is one preliminary bit of evidence that suggests that the electron configuration of the Fe^{III}−NO center might be better described as Fe^{II}−NO^{+}.[10]

The similarity in the Soret band position of the ferri- and ferroheme−NO centers of NP1−NO, and more especially, metMb−NO and Mb−NO,[20,21] are likely features of the optical spectra of other heme protein−NO complexes. If so, then it is important to point out that studies of the kinetics of nitric oxide synthase (NOS) that observe heme−NO intermediates *may* involve *either* Fe^{III}−NO (from which NO can dissociate with $K_d \sim \mu M$[13,17]) *or* Fe^{II}−NO (from which NO can dissociate much less readily, $K_d \sim$ pM[17]), and it may not be possible to differentiate these two oxidation states on the basis of Soret band position. The ability to differentiate between these two is crucial to developing a plausible mechanism for this enzymatic reaction.

A part of our original motivation for studying the electrochemistry of NP1 as compared to metmyoglobin was curiosity about the very different rates of autoreduction of the two proteins in the presence of high concentrations of NO: MetMbNO is autoreduced with a rate constant of 3.2×10^2 M^{-1} s^{-1} above pH 7, with a mechanism that requires a hydroxide ion in the rate-determining step and an additional NO molecule to complete the autoreduction.[46] Thus, the rate of autoreduction of metMbNO, and probably other ferriheme protein−NO complexes, depends on the concentration of OH^- and excess NO, and is thus quite slow if the pH is below neutral and the concentration of NO is very low. This may be the key for storage of NO in the *Rhodnius* insect, where the nitrophorins are in large concentration in the saliva glands but NO production in excess of the nitrophorin binding capacity is not expected to occur. We find that $NP1^{III}$−NO autoreduces only very slowly (over many hours to days) in the presence of high concentrations of excess NO, and as mentioned in the Results section, $NP1^{II}$−NO autoxidizes slowly in the absence of excess NO. It may be that the presence of a number of negative charges near the heme helps to slow the rate of autoreduction, by inhibiting the attack of OH^- on the bound NO.[46] Lack of change in the intensity of the infrared N−O stretching band over the pH range 5.5−9.5 over a period of up to 5 h indicates less than 3% autoreduction over this time period. $NP1^{III}$−NO could, however, be *photo-*

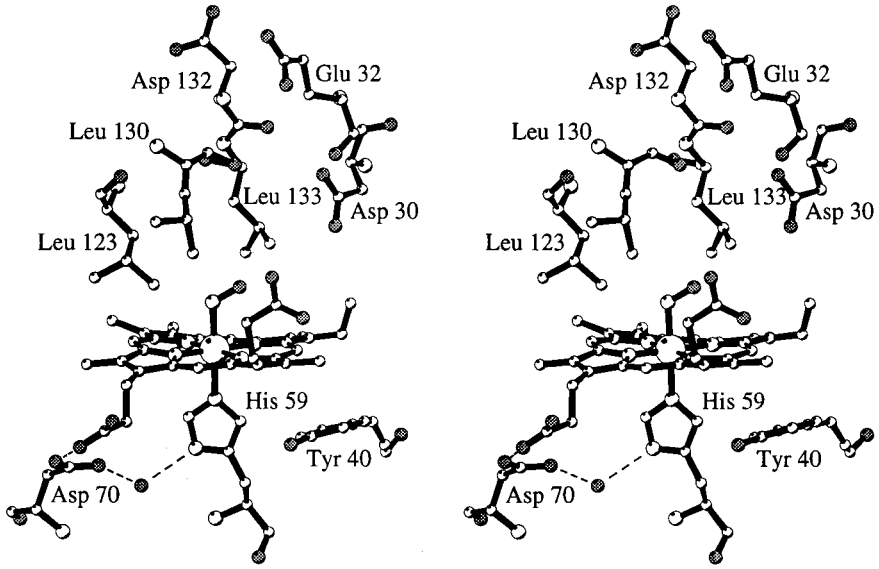

Figure 9. Stereoview of the heme-binding pocket, showing the proximal His-59, heme, bound NO, and nearby protein side chains. Oxygens are shown stippled, and nitrogens are drawn larger than carbons. Drawn with MOLSCRIPT.[71]

reduced to $NP1^{II}-NO$ by illumination with a visible light source in the presence of deazaflavin and EDTA. (See Experimental Section.)

In the present work, we have found that the reduction potentials of NP1 and metMb in the absence of NO differ by ~300 mV (Table 2), with NP1 having much less tendency to be reduced. The 300-mV difference corresponds to a $\Delta G°$ difference of 29 kJ/mol for the reduction half-reactions of the two proteins, with metMb having the more negative $\Delta G°$ and, hence, the greater tendency to be reduced. The same relative ease of reduction obviously applies to the NO complexes of the two proteins, although we cannot determine the difference in $\Delta G°$ because we cannot measure the reduction potential of metMb−NO. However, based on the data of Table 2, we can anticipate that the reduction potential of metMb−NO should be on the order of at least 300 mV more positive than that of $NP1^{III}-NO$, giving considerable driving force for the autoreduction of metMb by excess NO. Hence, at least a part of the reason for the difference in the ease and rate of autoreduction of the two proteins by NO rests in the differences in their reduction potentials; likely the remainder rests in the insulation of the $Fe^{III}-NO$ center from attack by OH^-, due to the multiple negative charges near the heme. (See ref 14 and Figure 8.)

The difference in reduction potential of NP1 and metMb in the absence of NO cannot be a result of a difference in ligation, since both proteins have a proximal histidine ligand, and unpublished NMR,[15] cyclic voltammetric,[47] and X-ray results indicate that NP1, like metMb, has a water molecule coordinated to the high-spin iron(III) center. Rather, the 300-mV difference in reduction potentials is most likely due to the difference in buried charges near the heme in the two proteins. The heme pocket of myoglobin is almost entirely lined with hydrophobic residues, apart from the distal histidine (E7) and threonine (E10).[48] A series of E11 valine mutants of myoglobin have been prepared by site-directed mutagenesis, including the Asn, Asp, and Glu mutants.[49] Replacement of Val E11 with Asn caused the reduction potential to be lowered by 83 mV, while replacement with Asp or Glu caused the potential to be lowered by much greater amounts (−191 and −196 mV, respectively).[49] In comparison, four potentially charged residues are in or near the heme pocket of NP1: Asp-30, which is near the heme (4.7 Å from the iron) and in the histamine complex forms a hydrogen bond to one of the histamine amino protons,[14] Glu-32 and Asp-34, which are near the surface of the protein on the distal side of the heme, and Glu-55 and Asp-70 on the proximal side (see ref 14 and Figure 8 below). Asp-70 makes a hydrogen bond to an ordered water molecule that in turn is hydrogen bonded to the proximal histidine ring $N_\delta H$ and is most likely uncharged. Most buried of all is Glu-55, which is at the back of the heme pocket.[14] Preliminary data on NP4 (90% sequence identity with NP1) indicate that this residue may have a pK_a of ~6.5,[50] however, and so Glu-55 is unlikely to have a major effect on the reduction potential of the heme, since the potential changes only slightly over the pH range 5.5−7.5 (Table 2). Asp-30 and Glu-55 are conserved among the four nitrophorins, and Glu-32 is conservatively replaced by Asp, while Asp-34 and Asp-70 are nonconservatively replaced by Gln and Asn, respectively, in NP2 and NP3.[51] Hence, there are a number of candidates for charged residues that may be responsible for the −300-mV shift in the reduction potential of NP1 as compared to metMb. Investigation of the electrochemistry of the other nitrophorins and of site-directed mutants of NP1 will be required to determine the importance of each. It should also be pointed out that there are two tyrosines (40 and 105) very near the heme on the proximal side, and a threonine (121) on the distal side,[14] which could also have some effect through formation of hydrogen bonds.

The minimal change in reduction potential (Table 2) over the pH 5.5−7.5 range (−15 mV/pH unit increase) argues against a change in protonation state of a key residue bound at or very near the heme over that pH range. Such a change in protonation would be expected to cause a change in potential of −59 mV per proton lost per pH unit,[52] if the key residue is very close to the heme iron. However, all of the above-mentioned carboxylates of NP1 are ≥8.5 Å from the iron, except for Asp-30. Evidence that there is a change in protonation of Glu-55 and a concomitant change in the electrostatics at the rear of the heme-binding pocket of NP4 over the pH range 5−7 will be published elsewhere.[50] However, these changes obviously do not have a major effect on the reduction potential (Table 2), probably because of the 10.1-Å distance between Glu-55 and the metal. The small (and similar) change in reduction potential of the heme center of myoglobin over the pH 5.5−7.5 range (−14 mV/pH unit increase, Table 2) has been observed by previous workers[53,54] and is believed to be because this pH range is between the acid pK_a of the heme propionates (<5), which cannot be studied by electrochemical techniques because of unfolding of the protein,[55] and the basic pK_a's of the heme (8.9 (bound H_2O deprotonation)[56] and ~10.5 (proximal histidine deprotonation)[57]). The similarity in pH dependence (Table 2) between myoglobin and NP1 suggests that NP1 is likewise between acidic and basic pK_a's of heme carboxylates, bound water, and histidine imidazole ring NH deprotonation over the pH range 5.5−7.5 and that this general medium effect is sufficient to explain the observed pH dependence of the reduction potential of NP1.

One currently unexplained aspect of NP1 reactivity concerns the pH dependence for NO binding, which is ~10-fold higher at pH 5 than at pH 8.3,[13] with an associated apparent pK_a of 6.5.[7] One would expect that a change in the reduction potential would accompany the change in binding affinity. However, only a minimal change was found (Table 2) over this range, and we have just interpreted that change as a general medium effect due to being between the acidic and basic pK_a's of the heme and its immediate ligands. The extrapolated change in reduction potential over 3.3 pH units (−50 mV) is sufficient to account for 60% of the change in $\Delta G°$ of NO release over this pH range. Previous data indicated a single titratable group was responsible,[7] which would mean that 90% of the change should occur over 2 pH units. This is not what has been found for the pure, recombinant protein,[13] suggesting that the earlier apparent pK_a findings[7] could have been the result of the presence of four nitrophorins of somewhat different pH dependences in the

(46) Hoshino, M.; Maeda, M.; Konishi, R.; Seki, H.; Ford, P. C. *J. Am. Chem. Soc.* **1996**, *118*, 5702.
(47) Houston, H. L. M.S. Thesis, University of Arizona, 1995.
(48) Takano, T. *J. Mol. Biol.* **1977**, *110*, 569.
(49) Varadarajan, R.; Zewert, T. E.; Gray, H. B.; Boxer, S. G. *Science* **1989**, *243*, 69.
(50) Weichsel, A.; Andersen, J. F.; Ding, X. D.; Balfour, C.; Walker, F. A.; Montfort, W. R. Manuscript in preparation.
(51) Champagne, D. E.; Ribeiro, J. M. C. Manuscript in preparation.
(52) Dryhurst, G.; Kadish, K. M.; Scheller, F.; Renneberg, R. *Biological Electrochemistry*; Academic Press: New York, 1982; Vol. 1, p 404.
(53) Taylor, J. F.; Morgan, V. E. *J. Biol. Chem.* **1942**, *144*, 15.
(54) Brunori, M.; Saggese, U.; Rotilio, G. C.; Antonini, E.; Wyman, J. *Biochemistry* **1971**, *10*, 1604.
(55) Mauk, A. G.; Moore, G. R. *J. Biocommun.* **1997**, *2*, 119.
(56) Brunori, M.; Amiconi, G.; Antonini, E.; Wyman, J.; Zito, R.; Fanelli, A. R. *Biochim. Biophys. Acta* **1968**, *154*, 315.
(57) (a) Walba, H.; Isensee, R. W. *J. Org. Chem.* **1956**, *21*, 702. (b) George, P.; Hanania, G. I. H.; Irvine, D. H.; Abu-issa, I. *J. Chem. Soc.* **1964**, 5689. (c) Yagil, G. *Tetrahedron* **1967**, *23*, 2855.

salivary gland homogenate. Additional studies will be required to resolve this point. In any case, NO release requires the electron configuration to be $Fe^{III}-NO^{\bullet}$ rather than $Fe^{II}NO^{+}$, so the direction and rough magnitude (within less than a factor of 2) of shift in reduction potential are consistent with the change in dissociation constant of the NO complex, $NP1^{III}-NO$.

The +428 to +430-mV shift in potential of the Fe^{III}/Fe^{II} reduction potential when NO is bound to the iron is a measure of the Fe−NO dissociation constants for the two oxidation sates, since, according to the Nernst equation,

$$E_c = E_o + (RT/nF)\ln(K_d^{III}/K_d^{II})$$

where E_c is the measured potential for the nitrophorin fully complexed to NO, E_o is the measured potential for the nitrophorin in the absence of NO, and K_d^{III} and K_d^{II} are the NO dissociation constants for the Fe(III) and Fe(II) states, respectively. The ratio of the dissociation constants for the two oxidation states is thus 22×10^6. The $Fe^{III}-NO$ dissociation constant has been measured at pH 5.0, 6.0, and 8.3.[13] Extrapolation to pH 5.5 and 7.5 gives $K_d^{III} = 0.347$ and 1 μM, respectively. Based on these values, the calculated $K_d^{II} = 20.8$ and 80.6 fM, respectively, at pH 5.5 and 7.5. In terms of *binding* constants, $1/K_d^{II} = 4.8$ and 1.2×10^{13} M^{-1}, respectively. These binding constants are larger (or dissociation constants smaller) by more than a factor of 10 than those for most other heme proteins.[17]

The EPR spectrum of Figure 4 indicates that the proximal histidine bond is easily broken, at least in the $Fe^{II}NO$ complex in frozen solution. This behavior of recombinant $NP1^{II}-NO$ is different than we reported previously for the salivary gland homogenate, which contained all four nitrophorins and showed only the EPR spectrum of the "base-on" complex, with His-59 coordinated.[7] Preliminary EPR studies of recombinant $NP4^{II}-NO$[15] suggest that it likewise easily loses its His-59 ligand. Hence, we suspect that either NP2 or NP3, or both, may be more easily reduced and more stable in the "base-on" $Fe^{II}NO$ state, so that the EPR spectra of these two NO complexes were observed for the salivary gland homogenate.[7] EPR studies of these proteins will be required to determine whether this is the case or not.

The infrared data presented in Figures 6 and 7 and summarized in Table 3 point out that the electronic properties and bonding in both the ferric and ferrous forms of NP1−NO are virtually identical to known complexes of heme proteins with diatomic ligands. Specifically, the infrared data confirm the hexacoordination of the ferrous−NO complex as seen by X-ray crystallography and (in part) EPR spectroscopy, as well as the 6-coordinate structure of the EPR-silent ferric−NO complex. The similarity is not confined to band position but also encompasses isotope shifts, appearance of more than a single band (see for example, ref 58), insensitivity of band positions to deuteration (not shown), and integrated intensities. However, the line widths observed are greater than average for CO, NO, and CN^- complexes of various heme proteins (4−33 cm^{-1} with an average of ~12 cm^{-1}).[12,22−25,59−62]

The mechanism leading to line broadening of the diatomic ligand stretching band seems to be operative regardless of the nature of the ligand (i.e., CO, CN^-, or NO). Line broadening may result from multiple conformations of the bound ligand, assisted by interaction with the aqueous solution and an unencumbered binding pocket.[60] Consistent with this possibility are line widths for several heme proteins with known crystal structures, for which we have inspected the extent of solvent exposure in space-filling representations using data from the Brookhaven Data Bank, of globins,[63] heme-containing enzymes[64] and nitrophorin 1 $NP1^{III}-CN$ (3NP1),[14] and $NP1^{II}-NO$ (4NP1) (this work)). The striking observation is that the nitrophorin CN^- (3NP1) and NO (4NP1) structures exhibit the highest solvent exposure of all heme proteins inspected. If one qualitatively defines the view of a half-sphere of one of the diatomic ligands as 100%, the other structures have exposures of 2−20% with the exception of the cyanide and reduced NO complexes of the *Escherichia coli* sulfite reductase heme protein, which have 40%, and the exposure of the cyanide and reduced NO complexes of NP1 is near 100%. Though this representation is an X-ray crystallographic (i.e., rigid) approach to possible solvent interaction (i.e., broadening of the infrared band of the diatomic), the inverse correlation between line width and solvent exposure is striking. The rotational mobility of the diatomic ligand in the generally hydrophobic pocket of the heme proteins may also contribute to the breadth of the diatomic stretching band. Access to the surface/solvent actually indicates freedom to move at least in this direction, so the difference between mobility and solvent access is partially superficial. The infrared data, representing dynamic averages in solution are therefore in full agreement with the high solvent exposure noted by Weichsel et al.[14] and this work, in the crystalline state.

Another possible reason for the broadened NO-stretching FTIR bands is that there may be a dynamic equilibrium (on the IR time scale) in aqueous solution at room temperature between the 6-coordinate (base-on) Fe−NO complex and a minor amount of the 5-coordinate (base-off) Fe−NO complex. Both of these forms are observed by EPR spectroscopy in frozen solutions of $NP1^{II}-NO$ (see above). Variable-temperature studies over a wide range of temperatures would be required to determine whether this factor is a contributor to the breadth of the NO-stretching band.

The β-barrel lipocalin fold of the nitrophorins, in particular for this work, NP1−NO (Figure 8), is a unique feature of the nitrophorin family of heme proteins, as mentioned previously for the NH_3, CN^-, and histamine complexes.[14] Heme protein structures reported previously for the globins, cytochromes, and others have had mainly α-helical structures. Lipocalins are known to be hydrophobic molecule carriers.[45] Several insect-derived lipocalins carry γ-biliverdin,[45c,d] which has been postulated to have been formed by a heme oxygenase-like reaction of coordinated hemin.[44]

Figure 9 shows the heme with NO and several key residues of the heme pocket. The heme is held in place by several close

(58) Jung, C.; Schulze, H.; Deprez, E. *Biochemistry* **1996**, *35*, 15088.
(59) Uchida, K.; Bandow, H.; Makino, R.; Sakaguchi, K.; Iizuka, T.; Ishimura, Y. *J. Biol. Chem.* **1985**, *260*, 1400.
(60) Maxwell, J. C.; Caughey, W. S. *Methods Enzymol.* **1978**, *54*, 302.
(61) Reddy, K. S.; Yonetani, T.; Tsuneshige, A.; Chance, B.; Kushkuley, B.; Stavrov, S. S.; Vanderkooi, J. M. *Biochemistry* **1996**, *35*, 5562.
(62) Sampath, V.; Rousseau, D. L.; Caughey, W. S. In *Methods in Nitric Oxide Research*; Feelisch, M., Stamler, J. S., Eds.; J. Wiley: Chichester, UK, 1996; pp 413−426.

(63) Globin structures used, and their PDB file names, are as follows: human recombinant hemoglobin cyanide, 1ABY.; elephant myoglobin cyanide, 1EMY.; sea hare myoglobin cyanide, 2FAL.; sperm whale myoglobin NO, 1HJT.; sperm whale myoglobin CO, 260K, 1MBC.; *Lupinus luteus* leghemoglobin CO, 1GDI.; *L. luteus* leghemoglobin NO, 1GDL.; *Scapharca inaequivalis* hemoglobin CO, 1SCT.; *Carretta carretta* myoglobin cyanide, 1LHT.; *Candina (Molpadia) arenicola* hemoglobin cyanide, 1HLM.
(64) Heme enzyme structures used, and their PDB file names, are as follows: *E. coli* sulfite reductase hemoprotein cyanide, 4GEP.; *E. coli* sulfite reductase hemoprotein deazaflavin/EDTA light reduced, NO, 6GEP.; *Pseudomonas putida* cytochrome $P450_{cam}$ CO, 3CPP.; *Arthromyces ramosus* peroxidase cyanide, 1ARU.

van der Waals contacts in addition to binding to the proximal histidine. A bent geometry of NO bound to Fe, with an Fe−N−O angle about 123 and 135° degrees for molecules I and II, respectively, was an unexpected finding. Such a geometry, characteristic of ferrous−NO complexes,[11] may be a result of photoreduction in the X-ray beam during data collection or of autoreduction of the ferric complex with excess of NO. In fact, we found that intensive soaking of NP1 crystals with a large excess of NO leads eventually (after several days) to the ferrous NO complex. Repeated attempts to obtain the structure of the Fe^{III}−NO complex, which should have a linear Fe−N−O unit,[12b] have thus far not been successful.

Despite the 2 mM concentration of NO used in soaking the crystals to produce the NO complex, there is no evidence of additional NO molecules in the crystal. The two disulfide bonds are intact, indicating that excess NO is not able to reduce these disulfide bonds to create thionitrosyl groups (RSSR + 2NO → 2RSNO). In the case of hemoglobin, thionitrosyl units formed oxidatively from the SH groups of Cys 93β are found to play an important role in lowering blood pressure.[65]

The partially open, hydrophobic, and spacious distal pocket of NP1, with a volume of ∼170 $Å^3$ [66] is lined with three leucines (123, 130, 133). NO is sandwiched between Leu-123 and Leu-133 (3.8 Å to each) and points along the β-meso heme position directly at Asp-30 (4.9 Å). Despite this, the NO moiety has higher exposure to the aqueous medium than do most other small-molecule complexes of heme proteins, as discussed above. Two other charged groups in close vicinity of the distal pocket, Glu-32 and Asp-34, are at somewhat greater distance from NO (10.5 and 9.0 Å, respectively, for molecule I, for which better electron density is observed) and are fully exposed to the solvent. Glu-55, another potentially charged residue, mentioned above in the discussion of the electrochemical results, is buried in the protein interior 10 Å away from the Fe atom. There is no distal histidine in this protein, unlike in most globins. The plane of the imidazole ring of His-59 in both molecules I and II is placed along the β,δ-meso direction of the heme and is almost coplanar with Fe−N−O on the other side of the heme. This orientation is stabilized by a water molecule that forms hydrogen bonds to the $N_\delta H$ of His-59 and to Asp-70, which is additionally hydrogen bound to the heme propionate. Since Asp-70 is buried and forms a hydrogen bond with the charged heme propionate, it most likely has a significantly elevated pK_a value and is uncharged at pH 7. The histidine N−Fe bond length of 2.0 Å clearly defines this as a base-on, 6-coordinate Fe^{II}−NO center, unlike the situation found for guanylyl cyclase, where binding of NO causes loss of the protein-provided ligand,[67,68] which in turn is presumed to cause a conformational change that initiates the cyclase enzymatic activity.[69,70] However, EPR spectra of frozen solutions of $NP1^{II}$−NO invariably show a mixture of 5- and 6-coordinate ferroheme−NO signals, as shown in Figure 4, suggesting that the histidine bond is at least weak and is readily broken when the protein is in solution, especially frozen solution.

The changes observed in the NMR spectrum of NP1−imidazole as a function of time following dissolution of lyophilized protein (Figure 5) suggest that the protein partially denatures upon lyophilization in such a way that the heme−His-59 bond is broken. Hence, when the protein is redissolved in buffered D_2O, the unsymmetrical protohemin prosthetic group binds with random orientation. However, because one orientation is highly preferred, the heme equilibrates over time to bind in the preferred orientation, as evidenced by the time dependence of the NMR spectrum, Figure 5. Similar behavior has been seen for other *b* heme-containing proteins, including bovine liver cytochrome b_5.[43] The structures of the protein determined thus far (this work and ref 14) clearly show a large number of phenylalanine and tyrosine aromatic rings packed around the vinyl and methyl substituents of the heme group in such as way as to create a very specific binding pocket for one, but not the other, heme orientational isomer.

Summary. Recombinant nitrophorin 1 readily binds NO in solution and in the crystalline state, but the protein is not readily autoreduced by excess NO. Optical spectra of Fe^{III}NO and Fe^{II}-NO of NP1 are extremely similar, and those of metMbNO and MbNO are even more similar, as reported previously,[20,21] which makes it difficult to characterize the oxidation state of the NO complex by UV−visible spectroscopy. The reduction potential of NP1 in the absence of NO is ∼300 mV more negative than that of metmyoglobin. In the presence of NO, the reduction potential shifts ∼+430 mV for NP1−NO, but the reduction potential of metMb−NO cannot be measured for comparison. These results are consistent with the difference in the rates of autoreduction of the two proteins. The reduction potential of the NP1−NO complex, along with previous measurements of the Fe^{III}−NO dissociation constant, allows estimation of K_d for Fe^{II}−NO as 20.8 and 80.6 fM at pH 5.5 and 7.5, respectively. The N−O stretching frequencies of $NP1^{III}$−NO and $NP1^{II}$−NO, measured by FTIR techniques, are very typical of other 6-coordinate heme−NO stretching frequencies in the two oxidation states. Both NMR and X-ray crystallography show that the protohemin center of NP1−imidazole has a very high preference for one orientation of the unsymmetrical protoheme moiety. The structure of NP1−NO is of the Fe^{II}−NO form of the protein, presumably formed by photoreduction in the X-ray beam. The proximal base, His-59, is clearly coordinated to the iron in the crystalline state (and at room temperature, according to IR data), but EPR studies show that part of the protein loses the histidine ligand in frozen solution.

Acknowledgment. This work was supported by the National Institutes of Health, Grant HL 54826 (F.A.W., W.R.M.), and The Netherlands Organization for Chemical Research (SON) with financial aid from The Netherlands Organization for Scientific Research (NWO). A.J.P. thanks Professors Siem Albracht (University of Amsterdam) and Wolfgang Buckel (Phillips Universität Marburg, Germany), who provided the opportunity to perform the FTIR experiments. The authors also thank Professor W. R. Scheidt for providing data prior to publication, and Professor J. S. Olson for helpful comments.

JA982979I

(65) (a) Jia, L.; Bonaventura, C.; Bonaventura, J.; Stamler, J. S. *Nature* **1996**, *380*, 221. (b) Stamler, J. S.; Jia, L.; Eu, J. P.; McMahon, T. J.; Demchenko, I. T.; Bonaventura, J.; Gernert, K.; Piantadosi, C. A. *Science* **1997**, *276*, 2034.

(66) Calculated using the GRASP program, with the NO and all solvent molecules temporarily removed from the cavity and two water molecules placed between Asp-34 and Leu-130 (on the surface of the protein molecule) to form a closed cavity.

(67) (a) Yu, A. E.; Hu, S.; Spiro, T. G.; Burstyn, J. N. *J. Am. Chem. Soc*. **1994**, *116*, 4117. (b) Dierks, E. A.; Hu, S.; Vogel, K. M.; Yu, A. E.; Spiro, T. G.; Burstyn, J. N. *J. Am. Chem. Soc.* **1997**, *119*, 7316.

(68) Stone, J. R.; Sands, R. H.; Dunham, W. R.; Marletta, M. A. *Biochim. Biophys. Res. Commun.* **1995**, *207*, 572.

(69) Ignarro, L. J.; Wood, K. S.; Wolin, M. S. *Adv. Cyclic Nucleotide Protein Phosphorylation Res*. **1984**, *17*, 267.

(70) Stone, J. R.; Marletta, M. A. *Biochemistry* **1996**, *35*, 1093.

(71) Kraulis, P. J. *J. Appl. Crystallogr*. **1991**, *24*, 946.

(72) Merritt, E. A.; Murphy, M. E. P. *Acta Crystallogr*. **1994**, *D50*, 869.

(73) Bacon, D. J.; Anderson, W. F. *J. Mol. Graphics* **1988**, *6*, 219.